Title

Characterization of expressed human meibum using hyperspectral stimulated Raman scattering microscopy

Journal

The Ocular Surface, 17(1)

ISSN

1542-0124

Authors

Paugh, Jerry R

Alfonso-Garcia, Alba

Nguyen, Andrew Loc

et al.

Publication Date

2019

DOI

10.1016/j.jtos.2018.10.003

Peer reviewed

HHS Public Access

Author manuscript

Ocul Surf. Author manuscript; available in PMC 2020 January 01.

Published in final edited form as:

Ocul Surf. 2019 January ; 17(1): 151–159. doi:10.1016/j.jtos.2018.10.003.

Characterization of expressed human meibum using hyperspectral stimulated Raman scattering microscopy.

Jerry R. Paugh, OD, PhD[1], **Alba Alfonso-Garcia, PhD**[2,3], **Andrew Loc Nguyen, PhD**[4], **Jeffrey L. Suhalim, PhD**[5], **Marjan Farid, MD**[6], **Sumit Garg, MD**[6], **Jeremiah Tao, MD**[6], **Donald J. Brown, PhD**[6], **Eric O. Potma, PhD**[2], and **James V. Jester, PhD**[5,6]

[1]Southern California College of Optometry at Marshall B. Ketchum University, Fullerton, California, USA

[2]Department of Chemistry, University of California, Irvine, Irvine, California, USA

[3]Current Affiliation: University of California at Davis, Department of Biomedical Engineering, Davis, California, USA

[4]Department of Mathematics, California State University Fullerton, California, USA

[5]Department of Biomedical Engineering, University of California, Irvine, California, USA

[6]Gavin Herbert Eye Institute, University of California, Irvine, California, USA

Abstract

Purpose: This study examined whether hyperspectral stimulated Raman scattering (hsSRS) microscopy can detect differences in meibum lipid to protein composition of normal and evaporative dry eye subjects with meibomian gland dysfunction.

Methods: Subjects were evaluated for tear breakup time (TBUT), staining, meibum expression and gland dropout. Expressed meibum was analyzed using SRS vibrational signatures in the CH stretching region (2800 – 3050 cm^{-1}). Vertex component analysis and K-means clustering were used to group the spectral signatures into four fractions containing high lipid (G1) to high protein (G4).

Results: Thirty-three subjects could be statistically analyzed using pooled meibum (13 with stable tear films (TBUTs > 10 seconds) and 20 with unstable tear films (TBUTs ≤ 10 seconds). Significant differences in meibum from subjects with unstable vs. stable TBUTs were found for the G1 fraction (medians 0.164 and 0.020, respectively; $p = 0.012$) and the G2 fraction (medians 0.244 and 0.272, respectively; $p = 0.045$). No differences were observed for the G3 and G4 fractions. Single orifice samples were not significantly different vs. pooled samples from the fellow eye, and eyelid sector samples (nasal, central and temporal) G2:G3 fractional components

Corresponding Author: Jerry R. Paugh, O.D., Ph.D., Southern California College of Optometry at Marshall B. Ketchum University 2575 Yorba Linda Blvd., Fullerton, CA 92831, Telephone: 714-449-7487, jpaugh@ketchum.edu, Facsimile: 714-992-7809.

The authors have no proprietary or commercial interest in any materials discussed in this article.

were not significantly different (p = 0.449). Spearman analysis suggested a significant inverse correlation between G1 fraction and TBUT (R = −0.351; p = 0.045).

Conclusions: hsSRS microscopy allows compositional analysis of expressed meibum from humans which correlated to changes in TBUT. These findings support the hypothesis that hsSRS may be useful in classifying meibum quality and evaluating the effects of therapy.

Keywords

dry eye; human meibum; machine learning; Raman spectroscopy

1. Introduction:

Dry Eye Disease (DED) is a common clinical condition, affecting 3 to 17% of the population, depending on the sampling approach and diagnostic criteria.[1] Two major forms of dry eye are recognized, aqueous deficient dry eye disease (ADDED) and evaporative dry eye disease (EDED) that are caused by dysfunction of the lacrimal gland and meibomian glands, respectively.

Of all dry eye, EDED caused by meibomian gland dysfunction (MGD) appears to be the more prevalent sub-type, accounting for as much as three times the prevalence vs. ADDED in one multicenter study.[2] However, whether ADDED or EDED, both sub-types exhibit significant and similar changes in the meibomian glands, including eyelid marginal changes,[3] expressibility decreases,[3] and gland dropout.[3, 4] Thus, understanding the fundamental mechanisms of pathologic changes in the meibomian glands becomes essential to understand and treat the broader cohort of dry eye conditions.

Histological studies in humans,[5] and animal models of induced MGD[6, 7] suggest central duct hyperkeratinization as one potential cause of gland dysfunction, leading to inspissated meibum secretions and eventual gland atrophy. However, increased viscosity of the meibum has been highlighted as another pathophysiologic mechanism in MGD,[8] although the mechanism leading to higher meibum viscosity is unclear. Studies evaluating the effect of temperature on meibum lipid conformation using infrared spectroscopy indicate that normal meibum is more disordered and fluid at eyelid temperature compared to meibum from subjects with MGD, which is more ordered and has a solid gel like phase.[9] These changes explain the appearance of increased meibum viscosity associated with MGD, and could be due to increased hydrocarbon chain length or saturation and changes in cholesterol ester content. Principal component analysis of normal and MGD meibum using infrared spectroscopy also identified changes in protein content, which may also affect meibum lipid viscosity.[10] The presence of keratin proteins in meibum lipids was first noted in an animal model of meibomian gland hyperkeratinization.[11] More recently, keratin proteins have been found to disrupt the normal structure of meibum lipid films, which may affect the evaporative function the tear lipid layer.[12] Proteomic analysis of meibum has identified over 90 proteins including keratins,[13] many of them playing roles in surface epithelial protection, lipid metabolism, inflammation and microbial infection.[14]

In a prior study using coherent anti-Stokes Raman scattering microscopy (CARS) and principal component analysis of mouse meibomian gland/eyelid tissue sections, Lin et al.[15] found spatial differences in the protein:lipid (P:L) profile that discriminated functional units of the meibomian gland, including the acinus, ductule and central duct. These spatial differences in the Raman vibrational spectra found between 2880 – 2940 cm^{-1} suggested the processing of meibum from the acinus prior to excretion onto the lipid margin. More rsecently, in a murine model of dry eye using desiccating stress, Suhalim et al.[16] used stimulated Raman scattering (SRS) microscopy to examine P:L ratios throughout the gland. In normal mice, Suhalim et al.[16] identified a progressive decrease in the P:L ratio from the acini to the central duct, confirming and extending the earlier findings of Lin et al.[15] By contrast, in the dry eye mouse model, the P:L ratio in the central duct was about 2-fold greater compared to the controls, suggesting that environmental stress may alter the normal maturation of meibum from the acinus to the orifice of the gland. While the mechanism and significance underlying meibum post-processing through the gland has yet to be discovered, these findings support the hypothesis that SRS analysis of meibum may be a sensitive tool for objectively characterizing the maturation state and quality of expressed meibum.

The purpose of this study was to determine whether hyperspectral SRS (hsSRS) microscopy could be used to characterize the P:L profile of expressed meibum and detect differences between normal and EDED subjects. The analysis of the hsSRS data involved a machine learning paradigm previously described,[17] which allowed a high-throughput, objective analysis of spectral data generated by a large number of samples. While that work explained in detail the methodology used, it is the scope of this study to use that methodology to further characterize human meibum samples and relate the hsSRS signatures to clinical parameters. For this report, three sub-studies were designed to investigate the basic variations in the Raman signatures of meibum expressed from orifices on different sectors of the same eyelid, between eyes, and between single orifice secretions and pooled secretions.

2. Methods

2.1 Subjects

Subjects included in this study comprised primarily a clinic-based sample. The study adhered to the tenets of the Declaration of Helsinki and all subjects provided written, informed consent following explanation of the nature and possible consequences of the study and prior to the administration of study procedures. The Institutional Review Boards of both the University of California at Irvine (UCI IRB HS#2015–2064) and Marshall B. Ketchum University approved the study protocol and conduct.

2.2 Inclusion, Exclusion Criteria

Subjects over age 18 were included, with no upper age or racial limitation. Subjects with and without dry eye symptoms were included so long as they did not use topical dry eye treatments on the day of examination. For this pilot study, subjects with aqueous deficient dry eye, assessed as an unanesthetized Schirmer result of < 5 mm in 5 minutes were excluded. Dry eye subjects were included “in progress” with their ongoing dry eye management, with the exception of the artificial tear use restriction. Subjects with mild

ectropion were included as well as those with prior contact lens wear so long as the lens wear was concluded six or more months prior to study examination.

Major exclusion criteria included ocular surgery less than 12 months prior to examination, ocular trauma in either eye within 6 months of examination, acute or chronic infection or uveitis, and concurrent use of topical medications for other indications such as glaucoma. Prior LASIK and cataract surgery patients were included so long as they adhered to the 12 months exclusion period. Also excluded were diabetics, women pregnant or lactating, and those with punctal plugs inserted within 30 days of examination. Persons with frank ectropion were also excluded.

2.3.1 Study Procedures, Clinical—Tests were administered from least invasive to more invasive.[18] Tear meniscus height for tear volume was measured using a reticule eyepiece, and white light interferometry was graded using the scale of Yokoi et al.[19] Global tests included fluorescein tear breakup time (TBUT; instilled 2.0 microliters of 1.0% wt./vol sodium fluorescein with micropipette; assessed with yellow filter for first dark spot appearance or change), and corneal and conjunctival staining using the N.E.I/Industry Workshop report[20] and the original Oxford system.[18] A yellow filter was also used for the staining assessment of sodium fluorescein.

Meibomian gland changes were assessed by examination of eyelid signs (1 if present, 0 if absent); orifice metaplasia, vascularity/brush marks, plugged orifices, ridging between orifices and margin irregularity, 0 – 5 scale). Meibomian gland secretion changes were assessed using a Q-tip along the entire lower eyelid margin with gentle pressure for 5 – 10 seconds, and secretion quality graded using the Foulks and Bron criteria[21] in 0.1 unit scale increments (scale range 0 – 3).

Gland atrophy was determined using meiboscopy of the entire lower eyelid,[3] counting the number of whole or half missing glands out of 24. This gave a percentage dropout (Grade 0 = no dropout; Grade 1 = ≤ 25% dropout, Grade 2 = ≤ 50% dropout, Grade 3 = ≤ 75% dropout, Grade 4 = 76 – 100% dropout). A Total MGD score was calculated by summing the eyelid margin score (0 – 5), the gland expression score (0 – 3), and the dropout score (0 – 4) for a total range of 0 – 12.

The Schirmer I test without anesthesia was conducted for tear production. The strip was left *in situ* for five minutes, but moved at 2 minutes to avoid false positives.[22]

2.3.2 Classification of Subjects into Stable or Unstable Tear Film—It was difficult in this study to cleanly assign subjects to either normal or MGD groups due to the overlap of MGD signs. For example, several subjects had normal or supra-normal tear breakup time values (i.e., > 10.0 to as much as 27 seconds), but who had meibomian gland secretion grades greater than grade 1.0 (cloudy or worse) and/or gland dropout by meiboscopy of greater than 1.0 (25% dropout). Since meibum is known to stabilize the tear film as demonstrated from deep gland expression in blepharitis subjects[23] and due to the evidence that TBUT as a diagnostic measure is felt to be an efficacious clinical test,[24, 25] we separated our sample into “stable” and “unstable” groups based solely on TBUT > 10.0 or ≤

10.0 seconds, respectively. The subjects in both stability groups were known to be non-aqueous deficient by Schirmer values > 5.0 mm of wetting.

The cut-point for stable vs. unstable tear stability is based on both expert panel recommendations[20, 26] and specific data from MGD subjects. Shimazaki et al.[27] found tear breakup times (TBUTs) of approximately 7 seconds (SDs of 5–6 seconds) for both normals and MGD subjects with solely orifice obstruction; TBUTs for greater changes such as gland dropout only or both dropout and orifice obstruction averaged 5–6 seconds.[27] Orifice obstruction is the initial step in gland dysfunction and later atrophy.[8] This evidence suggests that a reasonable upper limit for TBUT in MGD is ≤ 10 seconds.

2.3.3 Meibum Collection: Meibum was collected from both lower eyelids prior to the clinical stains being applied to the eye. With the subject behind the slit lamp biomicroscope at 10X magnification, the subject looked up and the lower eyelid was gently everted and the margin cleaned using a dry, sterile Q-tip in the central area. Then, a meibomian gland evaluator (MGE)[28] was used to apply constant pressure for 10 – 15 seconds. A sterile stainless steel foreign body spud (Miltex Ellis 18–380, Steele Supply Co., Michigan USA) was used to collect meibum from either single or several orifices. The meibum was smeared onto a clean microscope slide and stored at room temperature; see Figure 1. Two to four spectra were generated from each single smear.

The eyelid sector sub-study was conducted since sector differences in orifice meibum secretion have been noted,[28] and to examine the relative variability within a single eyelid. For the sector study meibum was collected from random subjects from the right eye only for each of the temporal, central and nasal eyelid regions and only one orifice was sampled. For the pooled samples, only the central 8 glands of the left eye of the same subject as the single orifice study were expressed using the MGE and typically 2–3 orifices were sampled. These pooled samples were compared to the central, single orifice of the right eyelid.

2.4 Hyperspectral stimulated Raman scattering microscopy and image processing:

A custom stimulated Raman scattering (SRS) microscope was used to acquire the hyper-spectral SRS (hsSRS) images as previously described.[16, 17] In brief, two picosecond laser beams were combined to drive selected vibrational modes of the sample in the CH-stretching region. The light beams were derived from a 76MHz mode-locked Nd:Vanadate laser (PicoTrain, High-Q, Hohenems, Austria) at 1064nm and a beam from a synchronously pumped optical parametric oscillator (OPO; Levante, Emerald OPO, Berlin, Germany) which can be spectrally tuned. Hyperspectral images were generated by sweeping the wavelength of the OPO output to tune the Raman shift from ~2800 to 3050 cm^{-1}, with 7 cm^{-1} intervals. The images were acquired on an inverted microscope (IX71, Olympus, Center Valley, PA, USA) using a 20× 0.75 NA objective lens (UplanS Apo, Olympus). Every hyperspectral image consisted of 512 × 512 (xy) pixels, with a lateral pixel size of 0.46 μm (unless otherwise indicated), each sampled at 37 spectral points. The stimulated Raman loss of the tunable OPO beam was detected by a photodiode (FDS1010; Thorlabs, Newton, NJ, USA) and custom electronics were used to process the signals. The power at the sample plane was kept below 30 mW to minimize photodamage.

The spectral analysis procedure has previously been described in detail[17], and is briefly summarized here. Using a training set of 19 images, originating from 17 unique subject samples, vertex component analysis (VCA) was employed to describe the acquired spectra as a linear combination of three basis spectra, representing RGB color components for visualization purposes; see Figure 2, A. The resulting spectral basis set featured spectra with prominent lipid (red) and protein (green) contributions. Subsequent K-means clustering analysis (KMCA) provided a coarse segmentation of the samples based on composition (Figure 2, B). Additional KMCA of the lipid-rich group identified four different spectral profiles that represent various mixtures of protein and lipids with progressively increasing P:L (G1-G4; Figure 2, C). Figure 2, D shows the process step by step from the maximum intensity projection of the hsSRS meibum image, to the VCA segmentation, followed by the KMCA steps.

Ultimately, a total of six spectral classes were defined, and used as reference spectra for a random forest classifier that categorized the remaining samples imaged for the study. This allowed high throughput of the recorded hsSRS images.[17]

2.5 Human Meibomian Gland Reference Spectra

To identify the presence of meibum post-processing in human meibomian glands, SRS microscopy was performed on human eyelid tissue obtained from a 71 year-old male collected under IRB approval (UCI IRB HS#2007–6050). Tissue was obtained during horizontal eyelid tightening surgery and the subject had no dry eye symptoms, but meiboscopy dropout grade of 1.0 (0 – 4 scale).[3] Tissue was embedded in O.C.T. Compound (Tissue-Tek, Torrance, CA), snap frozen in liquid nitrogen and cryo-sectioned using a Leica CM1850 cryostat (Leica Biosystems, Buffalo Grove, IL). Lipid-protein profiles were identified using SRS microscopy as previously described,[15] and signals averaged for the major regions of the meibomian gland (i.e., acini, duct, orifice and tissue matrix). As shown in Figure 3, there was a progressive reduction in the protein peak (i.e., 2930cm^{-1}) from the acini to orifice, which is similar to that observed in the normal healthy mouse meibomian gland.[15, 16]

From the spectral information obtained from the human meibomian gland, the spectral profiles from different regions of the gland appeared similar to the profiles identified from expressed meibum analyzed by hsSRS microscopy, such that G1 represents the orifice lipid-rich secretion, G2 and G3 the ductule fractions, and G4 the acinar protein-rich fractions.

2.6 Data Analysis

The spectral classification allows the identification the lipid content in the meibum smear, as well as the protein quantity mixed with the lipid on the micrometer scale. The protein to lipid variations across the different samples were the focus of this study. Regions devoid of lipid were excluded from the analysis. These regions were typically represented by spectra that resemble the spectrum of pure protein. Such areas might contain cellular debris and other components not related to expressed meibum. The background and pure protein components determined in the analysis were not considered in this study. The lipid components sub-divided into four groups (G1-G4) not only describe the sample's lipid

content, but also the lipid and protein interactions, and are therefore the components chosen to compare with the acquired clinical parameters described above.

Spectra of the lipid components from individual samples were normalized and tabulated as fractional values. The color scheme depicting the four lipid fractions, G1 – G4, in the images and the corresponding histograms were derived from the image processing procedure as detailed before.[17]

Statistical analyses of the lipid fractions were conducted using the clinical classification of stable tear films (TBUTs > 10.0 seconds) and unstable tear films (TBUTs ≤ 10.0 seconds). Data were checked for normality using boxplots and either parametric or non-parametric tests conducted. Correlational analyses examined associations between parameters and backward stepwise regression analysis was carried out to examine factors influencing tear stability.

3 Results

3.1 General Results

A total of 104 subjects were initially enrolled in this clinical study, with meibum collected from 56 subjects that was analyzed by hsSRS microscopy. The meibum collection procedure was comfortable with no reported adverse sequelae. Samples could not be reliably obtained in some cases due to gland atrophy or severe orifice capping.

A total of 33 subjects provided pooled samples from the left eyelid for statistical analysis. This sample had an age range of 18 – 89 years (average age 52.7 years; SD 18.6 years). Small sub-sets of samples were obtained to allow comparison of single orifices (right eyelid) to pooled samples from the fellow eyelid (left eyelid) and to compare single meibum fractions for a given eyelid.

3.2 Single Orifice vs. Pooled Orifice Comparison

Hyperspectral stimulated Raman scattering microscopic analysis of sampled meibum streaked onto glass slides showed a heterogeneous mixture of different protein to lipid fractions as shown in Figure 4. However, sampling of different regions within the sample indicated that the compositional profile of G1-G4 fractions were relatively consistent throughout the samples. Overall, the G2 and G3, putative ductule fractions, represented approximately the majority of the total lipid signal generated from the meibum smears (low fractional amount of 0.44 to high of 0.91; Figure 4). This was expected since the MGE is 5 mm in height and the length of the lower, central eyelid meibomian glands has been estimated at 2.0 mm.[8] Thus, the expressed meibum likely includes that resident in the ductules and distal portion of the central duct, a majority of the secretion.

We averaged the central, single orifice fraction data (2–3 scans) and compared to the pooled sample (2 −3 scans) from the left eyelid central orifices. Both samples were collected using the constant pressure of the MGE. The pooled meibum is what is available to the tear film and is probably the most representative of the two samples. The pooled fractional data serves

as the reference to the single orifice data from the right eyelid. Figure 5 illustrates the single vs. pooled orifice lipid fractional data.

There were no discernable trends in the average fractions of G2 combined with G3 for the single orifices (right eye) compared to the pooled samples from the central eyelid of the left eye. This was true even for eyelids who had meibum secretion grade differences (Bron scale[29]). For example, subject 63 had right single orifice combined G2 and G3 fraction of 0.83 (Grade 0.9 secretion quality) compared to G2 and G3 fraction of 0.67 (Grade 2.0 secretion quality) for the left eyelid.

Twelve subjects provided a central single orifice from the right eyelid to compare to the pooled fraction from the left eyelid. The G2:G3 fraction from the single orifice samples averaged 0.615 ± 0.23 as compared with an average of 0.719 ± 0.17 from the pooled fraction for the left central eyelid. These values were not significantly different (paired t-test; $p = 0.170$) suggesting that the single orifice G2:G3 fractions are similar to the pooled fractions.

3.3 Sector Comparisons, single eyelid:

For the eyelid sector sub-study, five subjects provided single orifice samples from the nasal, central and temporal sectors for comparison. To present the data simply, the G2 and G3 (ductule) fractions from each of the two analyses of the smear were averaged and are presented in Table 1 and Figure 6 for Subject 59. These fractions were the major fractions represented in the sample, likely due to the expression method, which expressed the entire gland length of the lower meibomian glands. The remaining fractions, G1and G4 behaved similarly.

Subjects 45 to 59 demonstrated consistent G2-G3 fractions, but subject 60 demonstrated a major difference for the temporal sector scans. Friedmans's test of the three sectors revealed no differences (medians of 0.656, 0.717, and 0.590 for central, nasal and temporal G2:G3 fractions, respectively; $p = 0.449$).

3.4 Repeatability:

Repeatability spectra were available for one subject under similar conditions two weeks apart. Figure 7 depicts the two image reconstructions and the corresponding fractional amounts for G1 – G4. The fractions shifted between the visits, as did the clinical grades (initially grade 2.7 (very thick, compromised meibum) in both eyes for the initial visit to grade 2.0 (opaque/cloudy with particles) in both eyes two weeks later). Whether this was a real alteration in the secretion quality as measured clinically and by hsSRS was not clear.

3.5 Stable vs. Unstable Tear Film Comparisons

Thirty-three subjects provided samples useable for analysis; 13 stable (TBUT > 10.0 seconds) and 20 unstable (TBUT ≤ 10.0 seconds). The lipid fraction data and relationships for this classification are summarized in Table 2 and the clinical parameters and relationships in Table 3.

The orifice meibum fraction, G1, and G2 (ductule faction) were significantly different ($p < 0.05$) in the stable and unstable groups and G3 (also ductule fraction) was borderline significantly different.

Spearman correlation analyses indicated that G1 fraction ($R = - 0.351$; $p = 0.045$), and G2 fraction ($R = 0.337$; $p = 0.055$) were significantly, or borderline significantly correlated with tear film breakup time (Figure 8 for G1). Also significantly correlated with TBUT were age ($R = -.402$; $P = 0.021$); NEI staining ($R = -0.383$; $P = 0.028$), and lower eyelid marginal signs ($R = -0.483$; $P = 0.004$).

Regression analysis, after adjusting for other factors such as age and sex was used to determine whether the lipid fractions G1 – G4 influenced tear film breakup time. In this small study group of 33 subjects, statistical analysis did not detect a significant influence ($P <.05$) of any lipid fraction on tear breakup time.

Additional step-wise regression analysis of demographic factors (age and sex) and clinical parameters to predict a stable tear film revealed that only lower eyelid marginal score (scale 0 – 5; 5 denotes all five margin signs present) was significant ($p < 0.01$). As a result, the prediction equation was:P (stable tear film) = exp (Y')/(1 + exp (Y')) where Y' = 4.29 – 1.212 (Lower Eyelid Margin Score). For example, using a score of 5 (worst score), the Y' becomes −1.77 and the probability (P) of a stable tear film becomes 0.145 (low probability). Except for lower eyelid margin score, none of the other factors evaluated showed a statistically significant influence on tear film breakup time, including meibomian gland expression grade, dropout and NEI fluorescein staining.

4 Discussion

The purpose of this study was to assess the ability of hsSRS microscopy to detect protein-lipid compositional differences in expressed human meibum collected from normal and EDED subjects. Our findings using this approach have several important implications for understanding meibomian gland function and its role in dry eye disease.

First, our data demonstrate that human meibum expressed from the meibomian glands contains a heterogeneous mixture of lipids that are complexed with variable amounts of protein as indicated by the increased CH_3 Raman spectral signature at 2940 cm^{-1}. Furthermore, using multivariate analysis and machine learning techniques, these heterogeneous profiles can be clustered into 4 different classes having either a low protein (G1) to high protein (G4) lipid content. By measuring the amount of each class within a sample, meibum can then be objectively characterized by the fractional composition of each lipid/protein class. While the specific nature of the protein to lipid interaction is unknown, the different lipid-protein signatures over the 2880–2940 cm^{-1} Raman spectra bear distinct similarity to different lipidprotein signatures from different regions of the meibomian gland evaluated in tissue sections. Namely, that the G1 fraction appears similar to that detected at the orifice and central duct of the human meibomian gland, while the G4 fraction appears similar to that detected at the acinus. We have detected similar spectral differences in the mouse meibomian gland from eyelid tissue sections,[15, 16] and our current findings support

and extend these observations to both human meibomian gland and meibum excreta expressed from human subjects.

We note that in the current analysis, we have excluded the regions in the meibum that are represented by Raman spectra similar to pure protein. In some samples, we observed significant protein-rich areas with spectra devoid of lipid contributions. These areas appeared phase segregated from the main, lipid-rich parts of the meibum excreta. In various cases, such protein clumps clearly resembled cellular debris, which likely originated from the epithelial surface of the eyelid and not from the expressed meibum. Based on this possibility it seemed justified to eliminate phase-segregated protein clumps from our analysis, while retaining all other components showing only complexed lipid and protein.

Proteins found in meibum have been implicated in protecting the tear film from bacterial invasion, lipid metabolism, as spreading agents and regulating the hydrostatic pressure of the tear film.[14, 30] Expressed meibum of human patients with MGD was found to contain elevated levels of protein,[10] and similar observations have been made in a mouse model.[16] It cannot be completely ruled out whether some of the protein contributions rejected from our analysis originated in fact from the meibum itself and have been phase segregated from the bulk during sample preparation. Therefore, it is possible that the exclusion of the pure protein component underestimates the total protein content of the meibum in the current analysis and explain in part the discrepancy between our findings and those of Borchman and co-workers[10] who identified elevated protein in meibum from MGD subjects.

Previously, we hypothesized that the differences in lipid-to protein content from different regions of the mouse meibomian gland represent maturation of meibum.[15] Our current SRS observations in human eyelid tissue sections suggests that a similar process may occur in the human meibomian gland. While we do not know what specific changes occur as meibum flows through the gland, future studies using imaging mass spectrometry[10, 31] of the meibomian gland may provide important clues to this process.

It is also interesting to note that the Raman spectral signatures of human meibum excreta had similarities to those identified in the human eyelid tissue sections. While we cannot know for certain the origin of the meibum excreta, it would be logical to assume that the different classes identified in excreta represent meibum expressed from different locations and depths within the meibomian gland. As such, it was initially surprising to find that the major lipid fractions (G2 and G3) appeared to originate from deeper within the gland and were less representative of meibum found at the orifice and central duct (G1).

In our study we used the meibomian gland evaluator (MGE), previously described by Korb et al.[28] to express the meibum. While the MGE exerts a constant force of 1.25g/mm^2, mimicking the force of a hard eyelid blink on the IOP, the area over which this force is applied is 8.76 mm x 4.5 mm and covers a linear extent of about 8 meibomian glands. Since the length of the meibomian gland in the lower eyelid from the eyelid margin to the base is only 2 mm,[8] and given that the application of force by the MGE is probably 1mm below the occlusal eyelid surface to avoid slipping onto the eye, most of this force would then be applied to the lower portion of the gland and not the anterior central duct. This would help

explain in part why much of meibum forcibly excreted from the gland shows distinct similarities to the lipid deeper within the gland, and not solely the anterior central duct. Of course, how lipid is secreted from the gland is not known and whether an expressor can ever mimic the exact application of forces seen by the meibomian gland during an eyelid blink is also not known. Nevertheless, it would appear that if maturation of meibum is important for normal meibum lipid function at the tear film, then the analysis of meibum through forced excretion may not be representative of the meibum that is secreted onto the tear film. This flaw in meibum collection may help explain some of the variability that is currently detected in the analysis of tear film lipid and meibum lipids from individual subjects.[32, 33]

Secondly, our study identified significant differences in the lipid fractions of meibum expressed from normal and EDED subjects. For the statistical and clinical analyses of these subjects, only pooled meibum samples from the left lower eyelid were analyzed (n = 33 unique subjects) rather than single-orifice meibum, since pooled meibum represents the meibomian lipids available to the tear film. Also, there did not appear to be any significant differences between single orifice samples or pooled samples, and there were no major differences between regional samples, i.e. nasal, central and temporal.

Using these pooled, central samples, G1, identified as meibum having a compositional similarity to meibum in the central duct of the gland in tissue sections and characterized by a Raman spectra showing the lowest protein, was found to have a larger fractional contribution (median 0.164) in subjects with shorter TBUT (<10s) compared to subjects with more stable TBUT (≥10s) (median 0.020). The G1 fraction also showed a significant inverse correlation with tear breakup time (R = - 0.351). Moreover, the G2 fraction, which had a greater protein to lipid composition than G1 and had a similar Raman spectra to meibum in the distal central duct and ductule in tissue sections, was lower in unstable tear film subjects (median 0.226) compared to stable tear film subjects (median = 0.272) and had a borderline significant positive correlation with tear breakup time (R = 0.337).

Overall, these findings appear contradictory to the concept that mature meibum, as represented by the G1 fraction, is important to the normal functioning of tear film lipid. However, this contradiction may have two possible explanations. First, it is generally thought that MGD is associated with obstruction of the meibomian gland orifice, leading to ductal dilation and a disuse acinar atrophy.[21] Based on this pathogenic mechanism, there should be more meibum lipid in the central duct of MGD subjects with EDED than normals, and therefore the fractional composition of G1 meibum should be higher in these subjects. However, it should be noted that in this study neither meibomian gland expression or meibomian gland dropout was significantly correlated with either changes in tear breakup time or the lipid fractions identified by hsSRS.

Alternatively, a second possibility is that gland atrophy and decreased lipid synthesis lead to reduced presence of G2-G3 meibum lipid fractions in EDED. As we have previously shown, age leads to a significant decrease in acinar cell cycling in both mice and humans,[34, 35] suggesting a decrease in meibocyte renewal and an overall decrease in meibum synthesis. Based on these findings, future clinical studies will need to be conducted that control for age

between normal and EDED subjects to more clearly identify the changes in meibum composition detected by hsSRS with altered tear film stability and EDED.

A clinical finding of note was that the lower eyelid marginal score (counted as “1” if present or “0” if not present; 0 – 5 scale for orifice metaplasia, orifice capping/plugging, ridging, telangiectasia and irregularity) was highly significantly different in the stable and unstable groups, and was significant in predicting a stable tear film by regression analysis. Arita and co-workers[24, 36] have reported high diagnostic test efficacy for these parameters. Taken together, this suggests that eyelid marginal signs, which are simple to observe and score, are very useful in the diagnosis of EDED related to MGD.

Finally, a somewhat surprising result of the study was the difficulty of assessing functional and morphological changes as indicators of MGD. We used the Bron scale[29] to grade expression quality, with a cloudy secretion (Grade 1.0) considered indicative of MGD. However, inspection of Table 3 demonstrates that a mean grade of 1.35 was found for secretion quality, supposedly pathological, in the thirteen subjects with TBUT > 10.0 seconds. These findings point to the need of improving the grading of meibum expression quality using more reliable measures of glandular function for the classification of MGD, e.g. hsSRS microscopy.

In summary, our results suggest that hsSRS may provide a sensitive and objective method for characterizing meibum quality, and for measuring the ratio of lipid to protein in expressed meibum. Since changes in meibum quality can lead to altered tear film stability and dry eye disease, more sensitive assays that categorize and classify meibum quality could greatly enhance our ability to diagnose disease and measure the efficacy of treatment. In this regard, understanding the chemical and molecular changes that give rise to the different lipid to protein classes identified in this report, will also expand our understanding of how meibomian gland function changes with age and disease. Specifically, given the difference in meibum that we have identified in this report using hsSRS, future research should explore different sampling approaches for spectroscopic assessment and grading of meibum. Additionally, concurrent compositional assays measuring altered lipids (e.g., O-acyl) ω-hydroxy fatty acid[30]) and proteins (e.g., insoluble keratinous particulates,[30, 37]and down-regulated normal proteins such as lacritin) in MGD subjects need to be undertaken to fully elucidate the relationships between fractional lipid and protein content relative to physiological behavior.

Conclusions:

Hyperspectral stimulated Raman scattering microscopy is a meaningful tool in detecting changes in meibum that might underlie the effects MGD on ocular tear film function and the development EDED. The hsSRS method enables compositional analysis of meibum in terms of lipid-to-protein content, a parameter of recent interest in MGD research. The lipid-to-protein fractions found by hsSRS microscopy correlate with TBUT, yet in an unexpected way, with the highest fraction of pure lipid (G1) found in subjects with unstable tear film. This study underlines both the usefulness of spectroscopic mapping methods like hsSRS in clinical assessment of meibum health, as well as the need for improved clinical assays for

expressed meibum collection to reduce compositional variations related to the expression procedure.

Acknowledgments

Supported in part by an Investigator Initiated Trial grant from Alcon Laboratories (JP), NEI EY021510 (JJ) and P41-RR01192 (EP and AAG), supported by an unrestricted grant from Research to Prevent Blindness, Inc., (RPB-203478), and the Skirball Program in Molecular Ophthalmology.

References:

1. Smith JA, Albietz J, Begley C, Caffery B,Nichols K, Schaumberg D, Schein O. The Epidemiology of Dry Eye Disease: Report of the Epidemiology Subcommittee of the International Dry Eye Workshop. The Ocular Surface 2007;5:93–107. [PubMed: 17508117]
2. Lemp MA, Crews LA, Bron AJ, Foulks GN, Sullivan BD. Distribution of aqueous-deficient and evaporative dry eye in a clinic-based patient cohort: a retrospective study. Cornea 2012;31:472–8. [PubMed: 22378109]
3. Pflugfelder SC, Tseng SCG, Sanabria O, Kell H, Garcia CG, Felix C, Fuer W, Reis B. Evaluation of subjective assessments and objective diagnostic tests for diagnosing tearfilm disorders known to cause ocular irritation. Cornea 1998;17:38–56. [PubMed: 9436879]
4. Shimazaki J, Goto E, Ono M,Shimmura S, Tsubota K. Meibomian gland dysfunction in patients with Sjogren syndrome. Ophthalmol 1998;105:1485–8.
5. Gutgesell V, Stern GA, Hood CI. Histopathology of meibomian gland dysfunction. Am J Ophthalmol 1982;94:383–7. [PubMed: 7124880]
6. Jester JV, Rife L, Nii D, Luttrull JK, Wilson L, Smith RE. In vivo biomicroscopy and photography of meibomian glands in a rabbit model of meibomian gland dysfunction. Invest Ophthalmol Vis Sci 1982;22:660–7. [PubMed: 7076409]
7. Ohnishi Y, Kohno T, Ishibashi T, Shinoda Y. [Macroscopic observation of the meibomian gland of the monkeys with experimental PCB intoxication]. Fukuoka Igaku Zasshi 1983;74:240–5. [PubMed: 6411566]
8. Knop E, Knop N, Millar T, Obata H, Sullivan DA. The International Workshop on Meibomian Gland Dysfunction: Report of the Subcommittee on Anatomy, Physiology, and Pathophysiology of the Meibomian Gland. Invest Ophthalmol Vis Sci 2011;52:1938–78. [PubMed: 21450915]
9. Borchman D, Foulks GN, Yappert MC, Bell J, Wells E, Neravetla S, Greenstone V. Human meibum lipid conformation and thermodynamic changes with meibomian-gland dysfunction. Invest Ophthalmol Vis Sci 2011;52:3805–17. [PubMed: 21398284]
10. Borchman D, Yappert MC, Foulks GN. Changes in human meibum lipid with meibomian gland dysfunction using principal component analysis. Exp Eye Res 2010;91:246–56. [PubMed: 20546726]
11. Jester J, Nicholaides N, Smith RE. Meibomian gland dysfunction I: keratin protein expression. Invest Ophthalmol Vis Sci 1989;30:927–35. [PubMed: 2470693]
12. Palaniappan CK, Schutt BS, Brauer L, Schicht M, Millar TJ. Effects of keratin and lung surfactant proteins on the surface activity of meibomian lipids. Invest Ophthalmol Vis Sci 2013;54:2571–81. [PubMed: 23482461]
13. Tsai PS, Evans JE, Green KM, Sullivan RM, Schaumberg DA, Richards SM, Dana MR, Sullivan DA. Proteomic analysis of human meibomian gland secretions. Br J Ophthalmol 2006;90:372–7. [PubMed: 16488965]
14. Jeyalatha MV, Qu Y, Liu Z, Ou S, He X, Bu J, Li S, Reinach PS, Liu Z, Li W. Function of meibomian gland: Contribution of proteins. Exp Eye Res 2017;163:29–36. [PubMed: 28950937]
15. Lin CY, Suhalim JL, Nien CL, Miljkovic MD, Diem M, Jester JV, Potma EO. Picosecond spectral coherent anti-Stokes Raman scattering imaging with principal component analysis of meibomian glands. J Biomed Opt 2011;16:021104. [PubMed: 21361667]

16. Suhalim JL, Parfitt GJ, Xie Y, De Pavia CS, Pflugfelder SC, Shah TN, Potma EO, Brown DJ, Jester JV. Effect of desiccating stress on mouse meibomian gland function. Ocul Surf 2014;12:59–68. [PubMed: 24439047]
17. Alfonso-Garcia A, Paugh J, FArid M, Garg S, Jester J, Potma E. A machine learning framework to analyze hyperspectral stimulated Raman Scattering microscopy images of expressed human meibum. J Raman Spectroscopy 2017.
18. Bron AJ, Evans VE, Smith JA. Grading of corneal and conjunctival staining in the context of other dry eye tests. Cornea 2003;22:640–50. [PubMed: 14508260]
19. Yokoi N, Takehisa Y, Kinoshita S. Correlation of tear lipid layer interference patterns with the diagnosis and severity of dry eye. Am J Ophthalmol 1996;122:818–24. [PubMed: 8956636]
20. Lemp M Report of the National Eye Institute/Industry workshop on clinical trials in dry eyes. CLAO J 1995;21:221–32. [PubMed: 8565190]
21. Foulks GN, Bron AJ. Meibomian gland dysfunction: a clinical scheme for description, diagnosis, classification and grading. The Ocular Surface 2003;1:107–26. [PubMed: 17075643]
22. Mackie IA, Seal DV The questionably dry eye. Br J Ophthalmol 1981;65:2–9. [PubMed: 7448154]
23. McCulley JP, Sciallis GF. Meibomain keratoconjunctivitis. Am J Ophthalmol 1977;84:788–93. [PubMed: 145804]
24. Arita R, Itoh K, Maeda S, Maeda K, Furuta A, Fukuoka S, Tomidokoro A, Amano S. Proposed diagnostic criteria for obstructive meibomian gland dysfunction. Ophthalmol 2009;116:2058–63.
25. Tse J Test efficacy of the fluorescein breakup time test in dry eye diagnosis [Masters Thesis]. Fullerton: Marshall B. Ketchum; 2014.
26. Sullivan BD, Whitmer D, Nichols KK, Tomlinson A, Foulks GN, Geerling G, Pepose JS, Kosheleff V, Porreco A, Lemp MA. An objective approach to dry eye disease severity. Invest Ophthalmol Vis Sci 2010;51:6125–30. [PubMed: 20631232]
27. Shimazaki J, Sakata M, Tsubota K. Ocular surface changes and discomfort in patients with Meibomian gland dysfunction. Arch Ophthalmol 1995;113:1266–70. [PubMed: 7575257]
28. Korb DR, Blackie CA. Meibomian gland diagnostic expressibility: correlation with dry eye symptoms and gland location. Cornea 2008;27:1142–7. [PubMed: 19034129]
29. Bron AJ, Benjamin L, Snibson GR. Meibomian gland disease. Classification and grading of lid changes. Eye 1991;5:395–411. [PubMed: 1743355]
30. Georgiev GA, Eftimov P, Yokoi N. Structure-function relationship of tear film lipid layer: A contemporary perspective. Exp Eye Res 2017;163:17–28. [PubMed: 28950936]
31. Anderson DM, Ablonczy Z, Koutalos Y, Spraggins J, Crouch RK, Caprioli RM, Schey KL. High resolution MALDI imaging mass spectrometry of retinal tissue lipids. J Am Soc Mass Spectrom 2014;25:1394–403. [PubMed: 24819461]
32. Brown SHJ, Kunnen CME, Duchoslav E, Dolla NK, Kelso MJ, Papas EB, de la jara PL, Wilcox MDP, Blanksby SJ, Mitchell TW. A comparison of patient matched meibum and tear lipidomes. Invest Ophthalmol Vis Sci 2013;54:7417–23. [PubMed: 24135754]
33. Brown SH, Kunnen CM, Papas EB, Lazon de la Jara P, Willcox MD, Blanksby SJ, Mitchell TW. Intersubject and Interday Variability in Human Tear and Meibum Lipidomes: A Pilot Study. Ocul Surf 2016;14:43–8. [PubMed: 26416436]
34. Nien CJ, Paugh JR, Massei S, Wahlert AJ, Kao WW, Jester JV. Age-related changes in the meibomian gland. Exp Eye Res 2009;E-pub ahead of print:doi.10.1016/j.exer.2009.08.013.
35. Nien CJ, Massei S, Lin G, Nabavi C, Tao J, Brown DJ, Paugh JR, Jester JV. Effects of age and dysfunction on human meibomian glands. Arch Ophthalmol 2011;129:462–9. [PubMed: 21482872]
36. Arita R, Minoura I, Morishige N, Shirakawa R, Fukuoka S, Asai K, Goto T, Imanaka T, Nakamura M. Development of Definitive and Reliable Grading Scales for Meibomian Gland Dysfunction. Am J Ophthalmol 2016.
37. Butovich IA, Lu H, McMahon A, Ketelson H, Senchyna M, Meadows D, Campbell E, Molai M, Linsenbardt E. Biophysical and morphological evaluation of human normal and dry eye meibum using hot stage polarized light microscopy. Invest Ophthalmol Vis Sci 2014;55:87101.

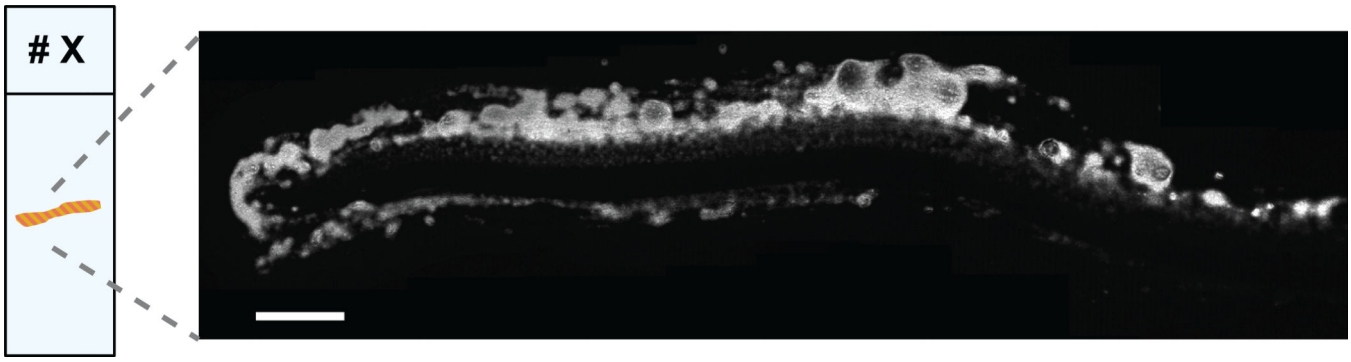

Figure 1.

Stimulated Raman scattering (SRS) microscopy provides chemical maps of the meibum streaks. The CH stretching region spans from 2800 cm^{-1} to 3100 cm^{-1}. Prominent features are the methylene (CH_2) vibrational mode at a Raman shift of 2850 cm^{-1} (above image), or the methyl (CH_3) vibrational mode at 2930 cm^{-1}. In hyperspectral SRS (hsSRS) the Raman shift is swept over the entire CH stretching region to reconstruct the Raman spectrum for every pixel in the image. A 512 × 512 image has 262,144 spectra per image. Lateral pixel size is 0.46 μm.

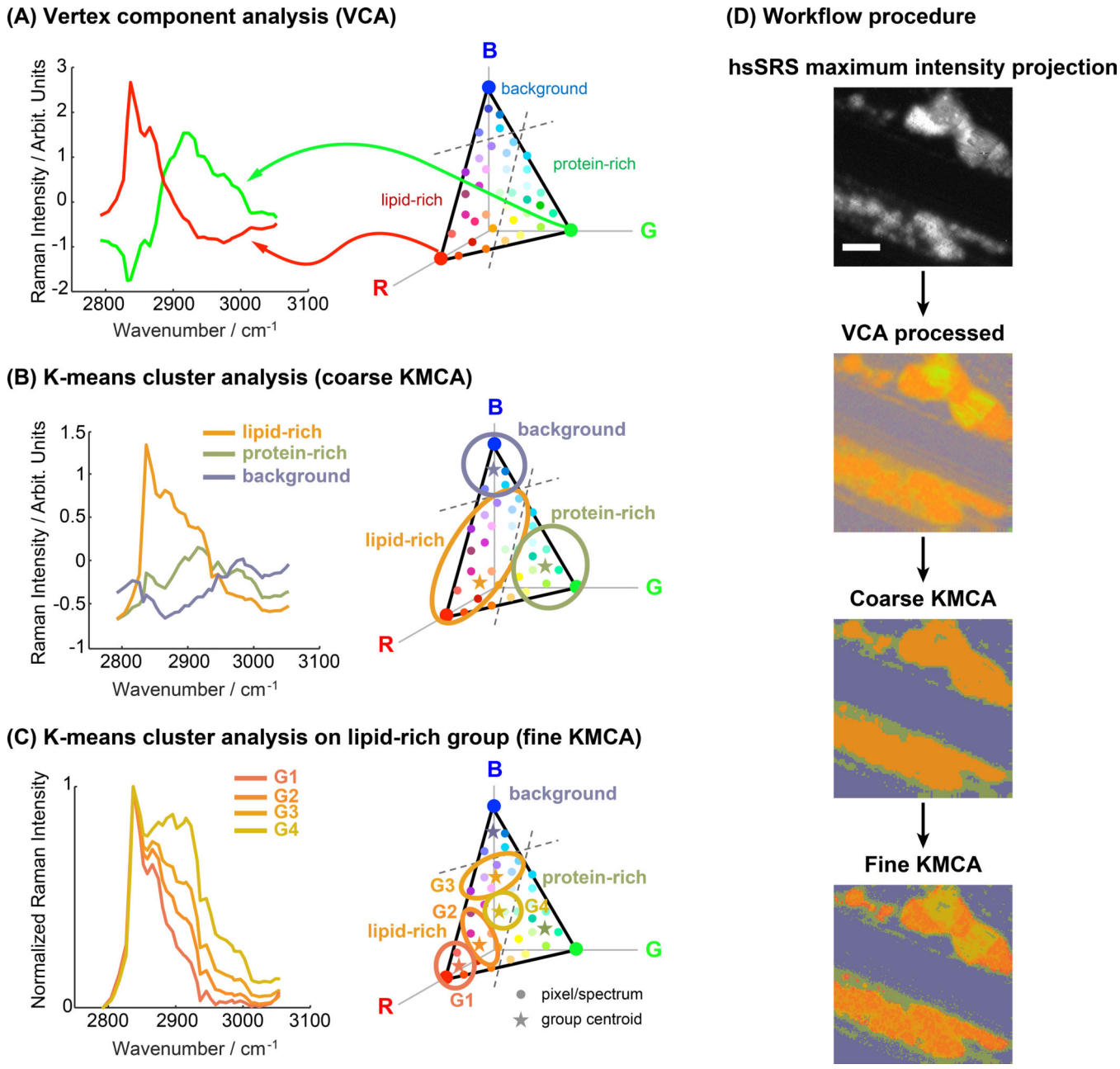

Figure 2.

Multivariate analysis characterizes the chemical composition of meibum samples. (A) Vertex component analysis (VCA) is used to describe the spectra in terms of three end members, each one assigned to an RGB base color. (B) The primary K-means clustering analysis (KMCA) groups the VCA output by color similarities and provides biochemical meaningful reference spectra. (C) A secondary KMCA within the lipid-rich group of the primary KMCA unveils additional clustering relevant to the protein-lipid composition of the meibum samples. D) Workflow of the image processing steps.

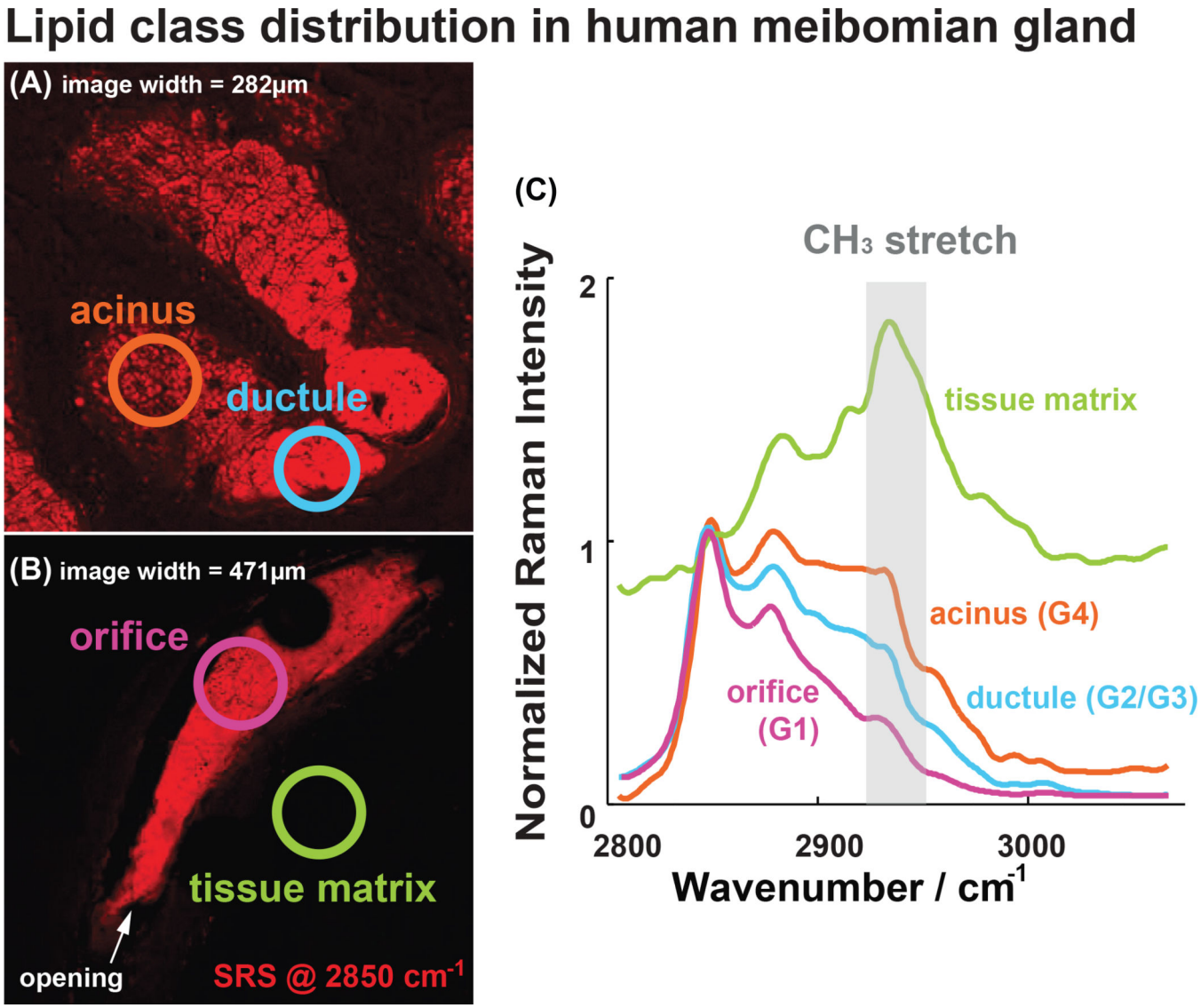

Figure 3.

Human meibomian gland shows a decrease of 2930 cm^{-1} CH_3 vibrational modes, also known as the protein band, from acini to orifice. (A) SRS image at 2850 cm^{-1} showing the acinus (orange circle) and the ductule (blue circle). (B) SRS image at 2850 cm^{-1} indicating the orifice (magenta circle) and a selected region of the tissue matrix (green circle). (C) SRS spectra of the indicated regions in (A) and (B). The spectral contribution near 2930 cm^{-1} decreases from the acinus to the ductule to the orifice.

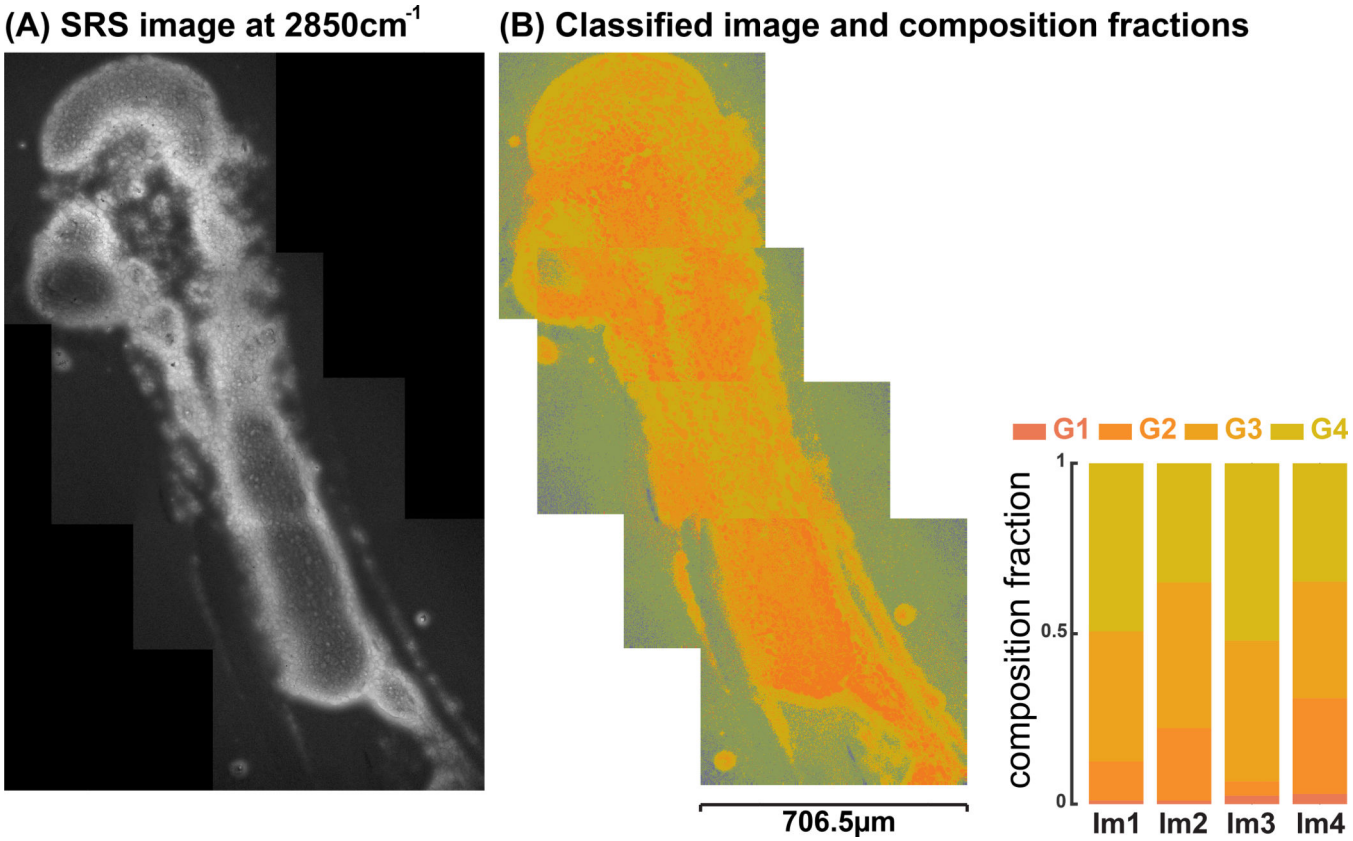

Figure 4.

(A) SRS mosaic image of an entire meibum secretion, with a lateral pixel size of 1.38 μm. (B) The corresponding spectral segmentation of the image in (A). The four meibum composition fractions are relatively consistent. Subject 106 had a lipid secretion grade 1.0 and was classified as clinically normal.

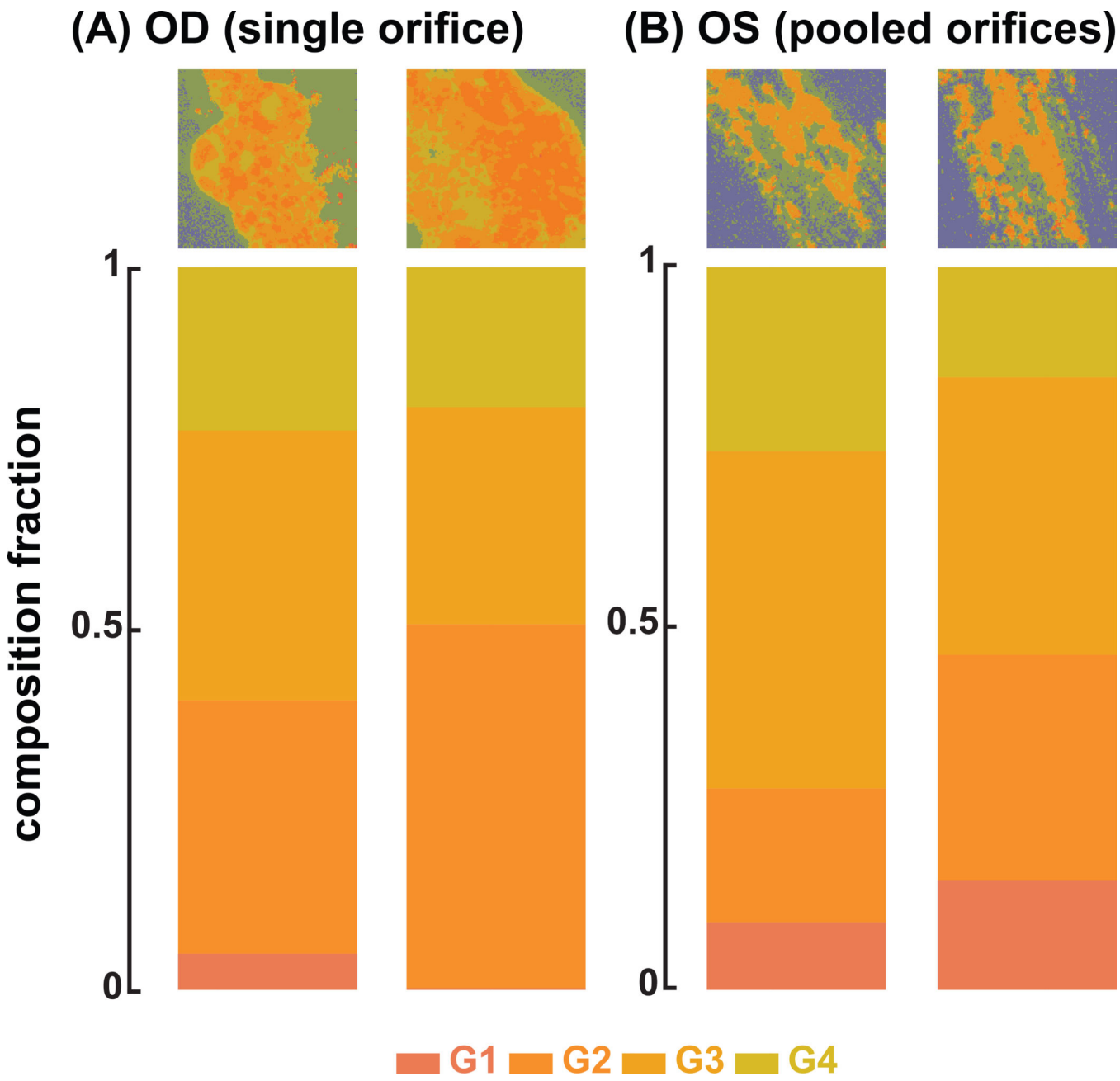

Figure 5.

Meibum fraction from single orifice from right eye (A) compared to pooled orifices (meibum from 2 or more orifices) in the left eye (B; both from the central eyelid sectors). Subject 62 was a 28 year old Caucasian male; lipid secretion grades 1.0 for right and left eyes, and classified as clinically normal.

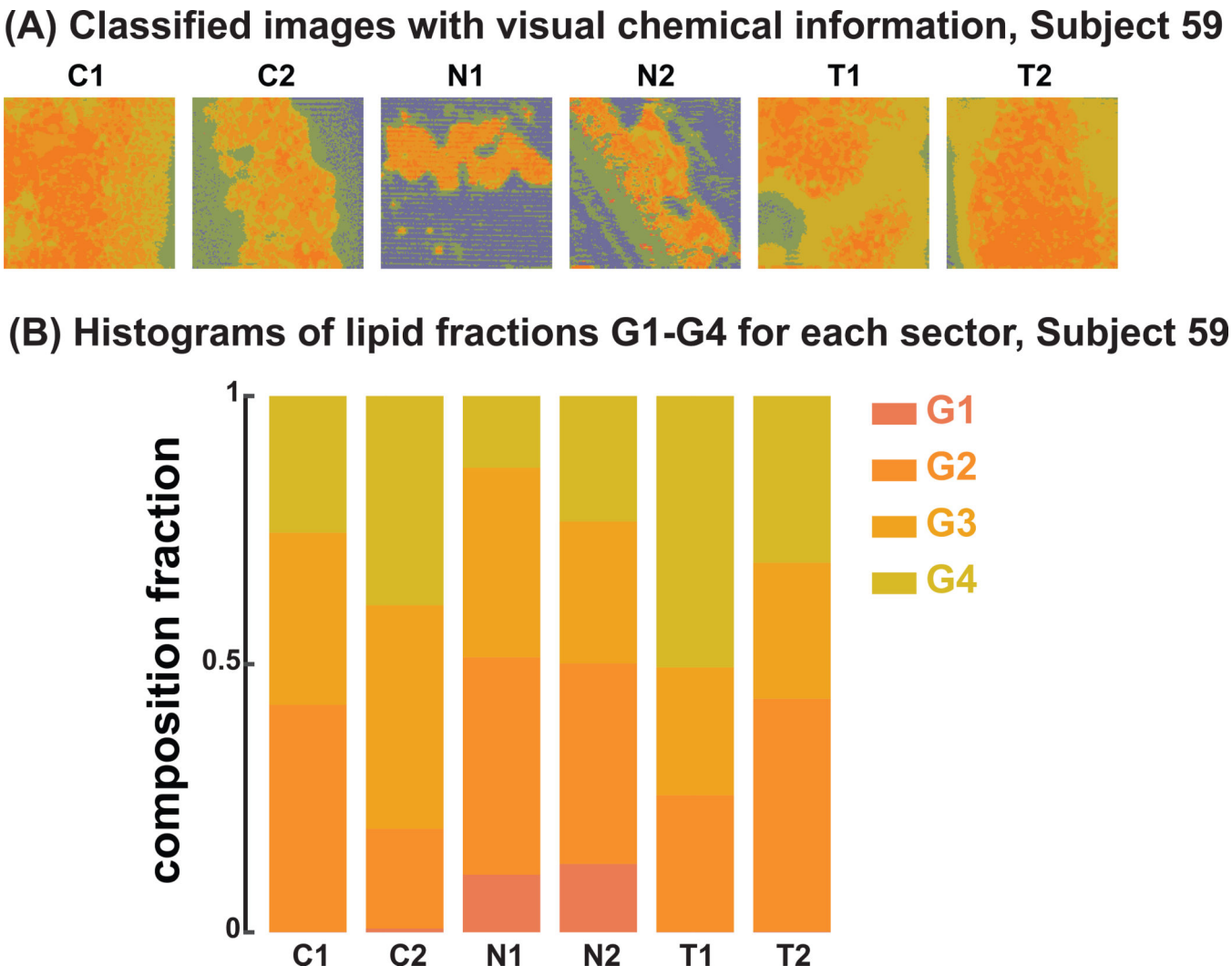

Figure 6.

Single orifice meibum fractions for one subject (right eyelid). “C” denotes central eyelid sector, N nasal, and T temporal. 1 and 2 denote two images from a single orifice. Subject 59 was a 69 year old Caucasian female; lipid secretion grade 1.2, and classified as having meibomian gland dysfunction (MGD).

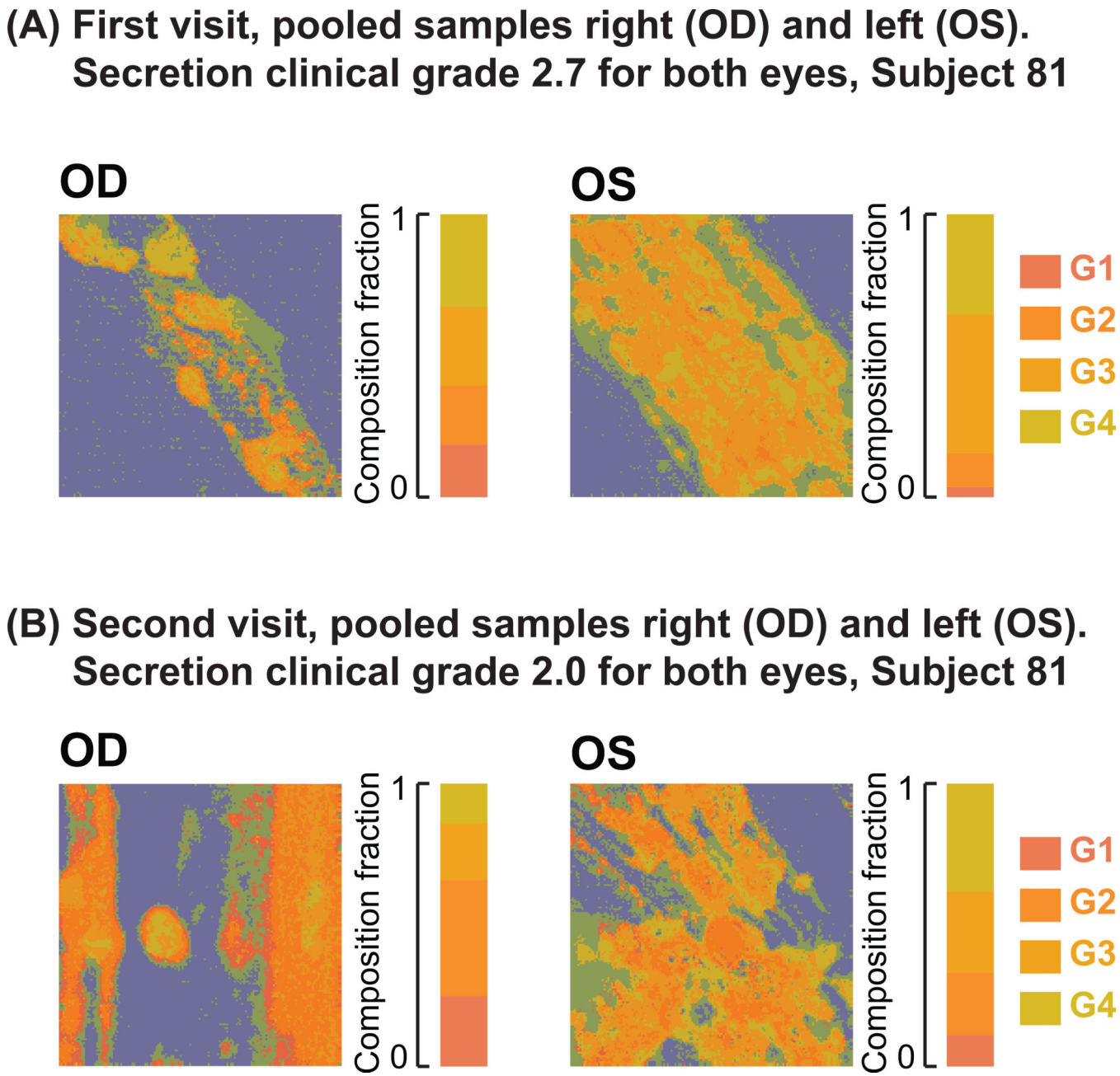

Figure 7.

Repeatability for one subject. Results from first visit (A) and second visit (B), two weeks apart. Subject 81 was a 50 year old Asian female; classified as MGD.

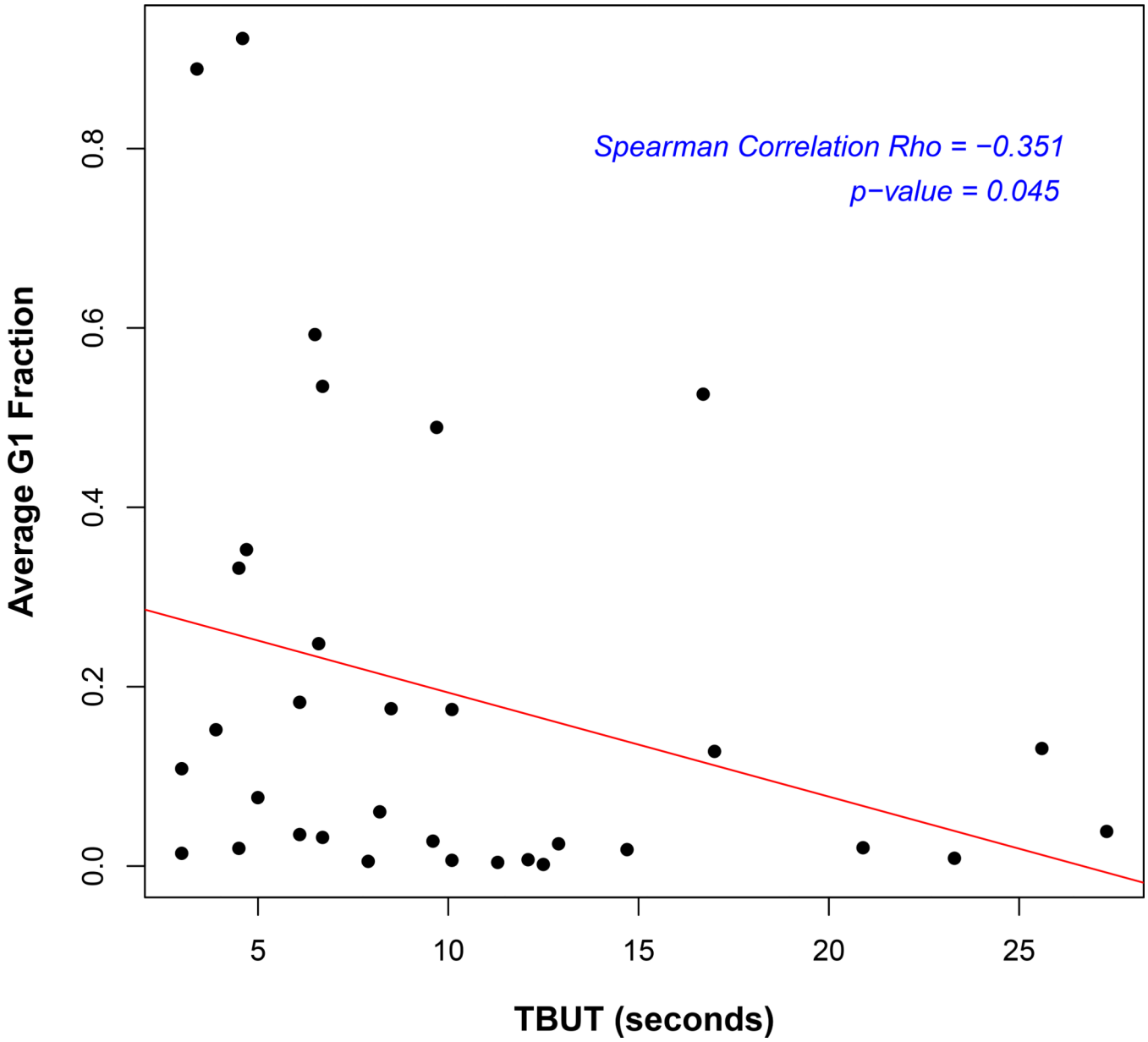

Figure 8.
Spearman correlation of G1 and tear breakup time. Apparent inverse relationship.

Table 1:

Fractional data for single orifices in three major eyelid sectors (R eyes only; 2 scans per smear; G2 and G3 fractions summed and averaged)

Subject	Secretion Grade*	G2-G3 Nasal	G2-G3 Central	G2-G3 Temporal
45	0.9	0.7653	0.8778	0.7759
46	0.5	0.7914	0.7126	0.6424
51	0.5	0.6555	0.5043	0.7711
59	1.2	0.6988	0.6740	0.5909
60	2.0	0.5711	0.4433	0.1706

*secretion grades 0 (clear, normal) to 3.0 (thick, inspissated). Grades ≤ 1.0 are normal; grades > 1.0 abnormal.

Table 2:

Meibum Fractions in Stable, Unstable Clinical Groups

Clinical Classification	G1 Fraction, mean (median) ±SD	G2 Fraction, mean (median) ±SD	G3 Fraction, mean (median) ±SD	G4 Fraction, mean (median) ±SD
Stable Tear Film (n = 13)	**0.084 (0.020)** 0.145	**0.316 (0.272)** 0.106	**0.426 (0.415)** 0.159	**0.174 (0.184)** 0.106
Unstable Tear Film (n = 20)	**0.263 (0.164)** 0.285	**0.244 (0.226)** 0.205	**0.304 (0.264)** 0.205	**0.190 (0.148)** 0.171
P-Value*	**0.012**	**0.045**	**0.074 (borderline)**	**0.811**

* Mann-Whitney U

Table 3:

Clinical Comparisons for Stable and Unstable

Parameter	Stable (n = 13), mean ±SD	Unstable (n = 20) mean ±SD	P-Value
Gland Expression (0 – 3)	**1.35** 0.5	**1.73** 0.5	0.048
Lipid Interferometry* (1–5)	**2.52** 0.8	**2.33** 0.5	**NS**
Lower Lid Margin Score (0 – 5)	**3.15** 1.1	**4.5** 0.9	0.002
NEI Staining (0 – 33)	**3.31** 2.1	**6.45** 3.9	0.005

* n = 8 stable, 18 unstable subjects; grading system of Yokoi et al, 1996[19]